*International Journal of Automotive Technology*, Vol. 23, No. 1, pp. 1–11 (2022)
DOI 10.1007/s12239–022–0001–6


pISSN 1229–9138/ eISSN 1976–3832

# FUEL DROPLET BEHAVIOR IN A CYLINDER UNDER THE DIFFERENCE $CO_2$ MOLE FRACTION CONDITIONS CONTROLLED BY SIMULATED-EGR IN CI ENGINE

Se Hun Min[1)] and Hyun Kyu Suh[2)*]

[1)]Department of Mechanical Engineering, Kongju National University, Chungnam 31080, Korea
[2)]Division of Mechanical and Automotive Engineering, Kongju National University, Chungnam 31080, Korea

*(Received 18 September 2020; Revised 23 October 2020; Accepted 2 November 2020)*

**ABSTRACT**–The objective of this numerical study is to investigate the effect of $CO_2$ mole fraction controlled by simulated-exhaust gas recirculation (EGR) on fuel droplet behavior for simultaneous exhaust emissions reduction in compression ignition engine under early injection conditions. In the simulation, the intake air initial composition was changed to simulate the EGR with changing $CO_2$ mole fraction. To consider early injection conditions, start of energizing timing was changed. The results were analyzed in terms of spray tip penetration, Sauter mean diameter, evaporated fuel ratio, and fuel mass fraction distributions. When $CO_2$ mole fraction increased, spray tip penetration was decreased because the kinetic energy of the injected fuel droplet was reduced by the high density of $CO_2$ and SMD was decreased since the high density of $CO_2$ disturbed the fuel progress, which induced the fuel droplet to have low kinetic energy. In addition, when the start of energizing timing was before top dead center 23 degree and $CO_2$ mole fraction was 20 %, exhaust emissions were expected to simultaneously reduce because the rapidly evaporated fuel by the collision effect promoted the combustion, and it made to evaporate the formed liquid wall film, which may absorb the combustion temperature by the latent heat vaporization.

**KEY WORDS** : $CO_2$ mole fraction, Fuel droplet behavior, Fuel mass fraction, Simulated-EGR exhaust emissions

## 1. INTRODUCTION

The reduction of exhaust emissions in a compression ignition (CI) engine is very important because the regulation for exhaust emissions is tightening (Regulation (EC) No. 715/2007, 2007). To reduce exhaust emissions, there are two representative methods.

First it is a method of reducing the combustion temperature, which suppresses the formation of emissions such as $NO_X$ (nitrogen oxide) at the region of high temperature (Pandey *et al*., 2019). Exhaust gas recirculation (EGR) is a representative method for decreasing the combustion temperature. It is to lower the oxygen concentration in the cylinder by recirculating some of the exhaust gas discharged from the internal combustion engine into the cylinder (Park and Bae, 2014). The low oxygen concentration in the cylinder decreases the combustion temperature by the deteriorated combustion performance, thus the $NO_X$ formation is suppressed (Hountalas *et al*., 2008; Kökkülünk *et al*., 2012) because the $NO_X$ is formed under the high temperature conditions (over 2,200K) (Turns, 2012). However, the low oxygen concentration in the cylinder also increases the emissions amount of soot, CO and so on, which is formed by incomplete combustion of the injected fuel (Shi *et al*., 2017).

Next, it is a method of homogeneously improving the air-fuel mixture in the cylinder. CI engine generates power from the auto-ignition of the injected fuel and combustion (Heywood, 1988). So, the homogeneous air-fuel mixture may reduce incomplete emissions such as soot, CO and so on. Lee and Reitz (2006) have conducted a study for targeting to reduce the soot and CO formation in premixed charge compression ignition (PCCI) combustion. As a result, the target of injected fuel was changed, which made the different distribution of air-fuel mixture, and it induced the different amount of exhaust emissions. Han *et al*. (2008) have reported the interesting results, which is that the wide spray injection angle improved the fuel atomization and the small hole diameter increased the rate of fuel evaporation. Park *et al*. (2011) have progressed a study to improve an air-fuel mixture by using a converging group-hole nozzle (cGHN). Fuel droplet injected form cGHN had high momentum and small Sauter mean diameter (SMD), which induces short combustion duration, as a result, the soot emission was reduced by homogeneously mixing the air-fuel mixture.

As well known, $NO_X$ and soot is the trade-off relationship, so the simultaneous reduction is very difficult. Cha *et al*. (2015) have conducted the experimental study to

*Corresponding author. e-mail: hksuh@kongju.ac.kr

simultaneously reduce the exhaust emissions by using the PCCI method under the different equivalence ratios. As a result, the $NO_X$ and soot emissions were decreased under the certain start of energizing timing and high equivalence ratio. Min *et al*. (2020) have reported that the $NO_X$ and soot emissions were simultaneously reduced when the start of energizing timing was around before top dead center (BTDC) 20 deg. These previous studies used only $N_2$ has to assume the EGR and adjusted the overall equivalence ratio. However, the actual EGR composed of $N_2$ and $CO_2$ and so on. Ladommatos *et al*. (1998) have conducted an experimental study to investigate the effect of $CO_2$ on the CI engine, and who reported that when $CO_2$ by EGR increased, nitro oxide emission was decreased because the temperature in the cylinder was decreased by a high specific heat capacity of $CO_2$. Furthermore, when $CO_2$ ratio in EGR increased, the matters by the incomplete combustion were raised because the equivalence ratio was increased by reducing of $O_2$ ratio in the cylinder according to the increment of $CO_2$.

As mentioned in the previous study, the properties of $CO_2$ such as specific heat, density, evaporation, and others are different from $N_2$, so it may occur the different results of spray characteristics from using only $N_2$ gas in the simulated-EGR. Liu *et al*. (2020) have presented interesting results. When the $CO_2$ concentration increased, the flame lift-off length was decreased because of the high $CO_2$ specific heat and the high density. Karaeen M. and Sher E. (2011) and Jin *et al*. (2008) have conducted the experimental studies for investigating the spray characteristics and announced that when $CO_2$ concentration increased, the spray tip penetration was decreased because the density of chamber was increased by the high density of $CO_2$ under the same ambient pressure.

As investigated in these previous studies (Ladommatos *et al*., 1998), the analysis of fuel droplet behavior such as Sauter mean diameter (SMD), spray tip penetration, evaporation, and so on is very important in CI engine because of the auto-ignition characteristic of fuel. As described above, the more homogeneous the air-fuel mixture becomes the more improved combustion characteristics and the less reduced exhaust emissions by incomplete combustion. Through spray tip penetration analysis, it is possible to find the optimal condition for the injected fuel to introduced into the hottest piston bowl in the cylinder. Moreover, through SMD characteristic analysis, it is possible to find the condition for having smaller droplets.

Although the optimal operation condition was suggested in the previous study to simultaneously reduce the exhaust emissions such as $NO_X$ and soot, only $N_2$ gas in simulated-EGR was used. In the study to investigate the effect of $CO_2$ on the CI engine, the effect according to $CO_2$ ratio on the CI engine under the same equivalence ratio did not accurately identify. Furthermore, the exact spray characteristics according to $CO_2$ amount were not able to confirm in the experimental study. Although the exact SMD values as time goes by and the number of droplet in the chamber are not able to be confirmed in experimental studies, it is possible in the numerical study.

Therefore, in this work, $CO_2$ was added to the simulated-EGR from the previous studies (Cha *et al*., 2015; Min *et al*., 2020), which used only $N_2$ gas, to assume closer the actual EGR. At the same time, the early injection conditions, which may occur the effect like the PCCI method, were applied to simultaneously reduce the exhaust emissions such as $NO_X$ and soot. Moreover, the effect of $CO_2$ mole fraction controlled by simulated-EGR on the fuel droplet behavior was investigated before the comparison and analysis of the combustion and exhaust emissions results according to the $CO_2$ mole fraction in a CI engine under early injection conditions. The fuel droplet behavior investigation is possible to predict the combustion performance and exhaust emissions characteristics. If the SMD of fuel droplet is large, it will not evaporate well and induce to form a lot of exhaust emissions by incomplete combustion. On the other hand, the small SMD of fuel droplet will evaporate well, it induces to evenly distribute the fuel mass fraction in the cylinder. For these reasons, this study performed an accurate analysis of the exact fuel droplet behavior according to the amount of $CO_2$ by simulated-EGR before the investigation of the combustion and exhaust emission characteristics of CI engine.

So, in this study, the effect of $CO_2$ mole fraction on the fuel droplet behavior under the different early injection conditions was investigated for finding the optimal conditions and reason to simultaneously reduce the exhaust emissions. At the same time, the results of spray characteristics were analyzed in terms of SMD, evaporated fuel ratio, and equivalence ratio distributions. In addition, the distributions of fuel mass fraction in the cylinder were compared and analyzed to observe air-fuel mixture according to the $CO_2$ mole fraction by using the engine simulation.

## 2. EXPERIMENTAL AND NUMERICAL DESCRIPTIONS

### 2.1. Experimental Setup

The experiment was progressed to validate the numerical analysis and the experimental apparatus consisted of a common-rail injection system, an Ar-ion laser, an intensified charge-coupled device (ICCD) camera, and a high-pressure chamber as shown in Figure 1.

The used test injector is mini sac type, 156 ° of inclined spray angle, 0.128 mm hole diameter and 6 hole nozzle. The injection pressure and the ambient pressure in the chamber were adjusted by 100 MPa, and 4 MPa, respectively. The required injection rate for simulation was measured by using Bosch's suggestion (Bosch, 1966) as

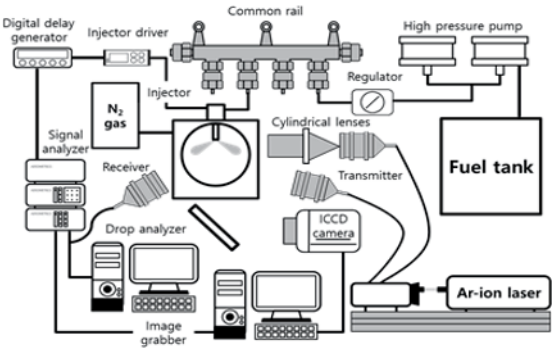


Figure 1. Schematic of experimental apparatus.

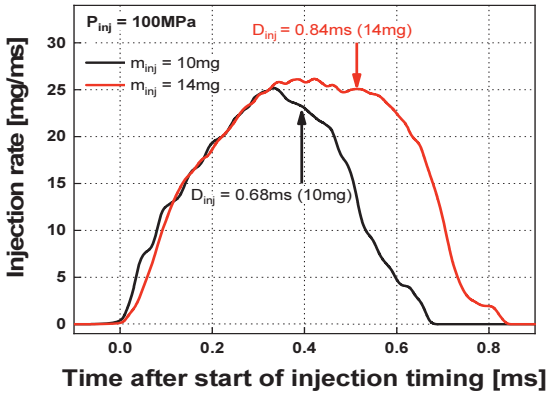


Figure 2. Injection rate according to the injection mass.

shown in Figure 2. Two injected fuel masses were applied at 10 mg (injection duration ($D_{inj}$) = 0.68 ms), and 14 mg ($D_{inj}$ = 0.84 ms) because a lot of fuel injection mass was difficult to observe the spray evolution. So, the injection mass of 10 mg was used for spray validation, and the 14 mg was employed for engine simulation considering the test results.

## 2.2. Numerical Setup

In this work, two-part of numerical analysis was conducted. First, the spray simulation was progressed for validating the spray characteristics, and the engine simulation was conducted for analyzing the air-fuel mixture formation according to the $CO_2$ mole fraction under the different start of energizing timing ($t_{eng}$).

To validate the spray characteristics, the chamber mesh of cylinder shape was used, whose diameter was 140 mm, and the height was 50 mm. To conduct the engine simulation, the used engine mesh were shown in Figure 3. The engine mesh for the engine simulation was generated only 1/6 of whole cylinder geometry for improving the accuracy and reducing the computational time.

Table 1 (AVL GmbH, 2013) lists the sub-model, which were applied to express the physical and chemical phenomena in the numerical analysis. Wall interaction

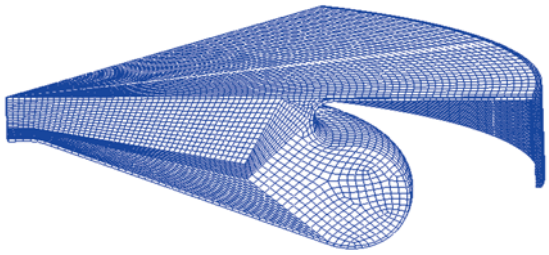

Figure 3. Geometry of engine mesh.

Table 1. Sub-model for simulation (AVL Gmbh, 2013).

| Phenomenon | Model |
|---|---|
| Turbulence | k-zeta-f |
| Evaporation | Dukowicz |
| Wall interaction | Mundo-Tropea-Sommerfeld |
| Break-up | Wave |

model was employed Mundo-Tropea-Sommerfeld because the occurrence of liquid wall film was expected by the early injection timing. Mundo-Tropea-Sommerfeld model consisted of the splashing regime and the deposition regime by the splashing parameter (K) as the following Equation (1).

$$K = \sqrt{We\sqrt{Re}} = Oh\, Re^{1.25} \tag{1}$$

If the splashing parameter (K) value is less than 57.6, the injected fuel droplet occurs deposition, whereas the splashing parameter (K) value is 57.6 or more, the injected fuel droplet occurs splash. When the splash occurs, the different diameter, velocity, and mass according to the wall roughness. If the hitting wall of the injected fuel is smooth, the following Equations (2) ~ (5) are used.

$$\frac{m_o}{m_i} = 3.9896 \cdot 10^{-21} K^{9.2133} \tag{2}$$

$$\frac{d_o}{d_i} = 0.88 - 0.013 \cdot K^{0.8} \tag{3}$$

$$\frac{v_{to}}{v_{ti}} = 1.068 \tag{4}$$

$$\frac{v_{no}}{v_{ni}} = 0.208 \tag{5}$$

On the contrary, if the hitting wall of the injected fuel is rough, the following Equations (6) ~ (9) are employed.

$$\frac{m_o}{m_i} = 8.035 \cdot 10^{-11} K^{9.2133} \tag{6}$$

$$\frac{d_o}{d_i} = 0.43 - 0.003 \cdot K^{0.9} \quad (7)$$

$$\frac{v_{to}}{v_{ti}} = 0.965 \quad (8)$$

$$\frac{v_{no}}{v_{ni}} = 0.407 \quad (9)$$

Here, "i" and "o" denote incoming and outgoing, "t" and "n" represent tangential and normal, respectively.

In the spray simulation, to match the experimental condition, the injection pressure and ambient pressure were applied as 100 MPa and 4 MPa, respectively. Diesel-D1 ($C_{13}H_{23}$) was employed for the test fuel in the simulation by referring to the library in the used program (Cengel and Boles, 2011). As described above, the injection mass was employed into two parts as 10 mg and 14 mg. To validate the numerical result, 10 mg was used in the spray simulation, and then the reliability was secured through the comparison of the results of 10 mg and 14 mg. To validate the numerical result, 10 mg was used in the spray simulation, and then the reliability was secured through the comparison of the results of 10 mg and 14 mg. The detailed spray simulation condition is listed in Table 2.

In the engine simulation, the EGR effect was expressed by the simulated-EGR, which was controlled through the initial air composition in the cylinder. The overall equivalence ratio was fixed by 0.68, which is the optimal operating conditions suggested in the previous study (Min *et al*., 2020), it was adjusted by decreasing the $O_2$ concentration from 21 % to 16.2 %. The $CO_2$ mole fraction in the cylinder was varied from 0 % to 20 %, the start of energizing timing was changed from BTDC 11 deg to BTDC 29 deg, and the detailed engine simulation conditions are listed in Table 3.

Table 2. Detailed spray simulation conditions.

| Phenomenon | Condition |
|---|---|
| Injection pressure [MPa] | 100 |
| Ambient pressure [MPa] | 4 |
| Injection mass [mg] | 10, 14 |

Table 3. Detailed spray simulation conditions.

| RPM | | | 1,200 |
|---|---|---|---|
| Injection pressure [MPa] | | | 100 |
| Injection mass [mg] | | | 14 |
| Start of energizing timing [ATDC deg] | | | -29, -26, -23, -20, -17, -14, -11 |
| Equivalence ratio [-] | | | 0.68 |
| Overall equi. ratio [ϕ] | $CO_2$ mole fraction [%] | $O_2$ mole fraction [%] | $N_2$ mole fraction [%] |
| 0.68 | 0 | 16.2 | 83.8 |
| 0.68 | 5 | 16.2 | 78.8 |
| 0.68 | 10 | 16.2 | 73.8 |
| 0.68 | 15 | 16.2 | 68.8 |
| 0.68 | 20 | 16.2 | 63.8 |

## 3. RESULTS AND DISCUSSIONS

### 3.1. Validation of Numerical Models

In this study, the numerical model has verified the reliability by comparing the experiment results, which obtained under the same conditions. To secure the reliability of the numerical model, experiments under two ambient pressure conditions as 3 MPa and 4 MPa were conducted. As described above, two times of spray simulation were

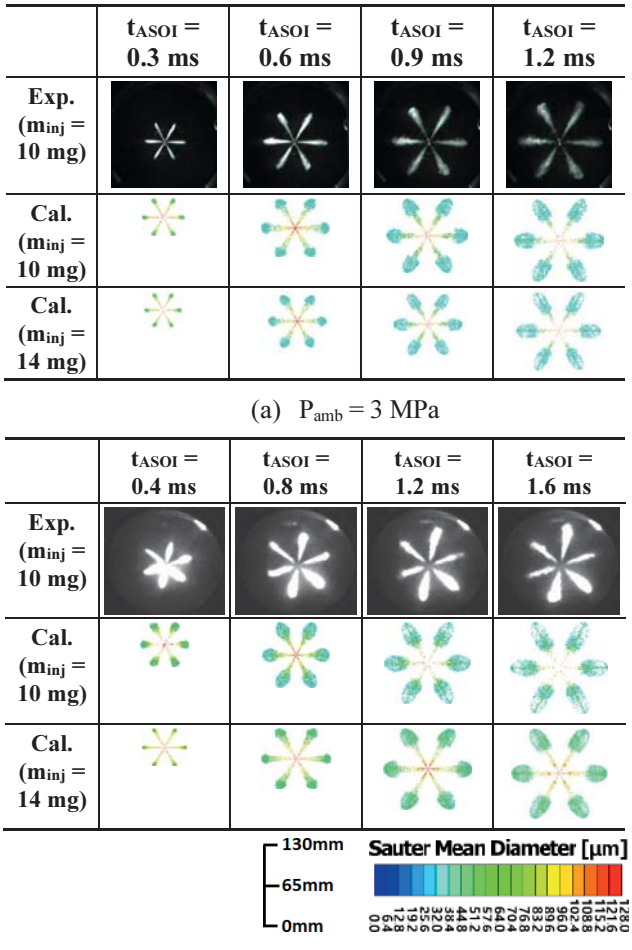


Figure 4. Validation results of spray evolution characteristics ($P_{inj}$ = 100 MPa).

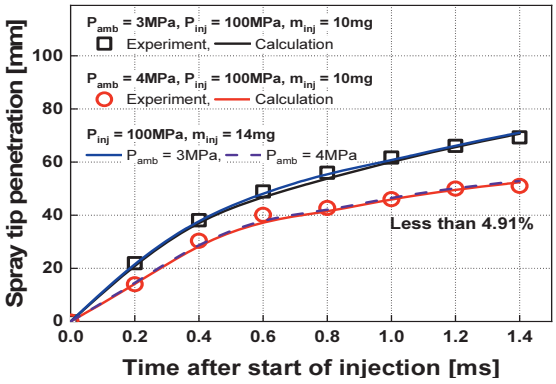


Figure 5. Validation results of spray tip penetration ($P_{inj}$ = 100 MPa).

conducted as 10 mg and 14 mg. The injection mass of 10 mg was used to obtain the spray factors such as spray cone angle and spray tip penetration, and these obtained spray factors were employed to the 14 mg, which was applied to the engine simulation. Since the different injection masses for the spray validation and the engine simulation, they could induce different results, so the relationship between these different injection masses was also confirmed.

Figures 4 and 5 show the comparison of the experimental and numerical results for spray evolution characteristics and spray tip penetration characteristics. The spray evolution characteristic is shown in Figure 4. In the validation of spray evolution characteristics, the spray cone angle validation was also conducted. To match the spray cone angle in the simulation with the experiment result, the spray cone angle was changed by 1deg from 0 deg to 20 deg and measured. At the same time, in the break-up model (Wave model), the break-up time control parameter ($C_2$) value was varied to find the optimal spray cone angle as the spray shape. Wave model has the following Equation (10), it is heavily influenced by the $C_2$ value.

$$\frac{dr}{dt} = \frac{(r_{stable} - r)}{\tau_a} \tag{10}$$

Here, $r_{stable}$ is the droplet radius of the product droplet, which is proportional to the wavelength $\Lambda$ of the fastest growing wave on the liquid surface. $\tau_a$ denotes the break-up time, it has the following Equation (11).

$$\tau_a = \frac{3.726 \cdot C_2 \cdot r}{\Lambda \cdot \Omega} \tag{11}$$

Here, $C_2$ means break-up time control parameter. $C_2$ is very sensitive parameter, if the $C_2$ value increases, the break-up late occurs, $C_2$ value decreases, the break-up quickly occurred. Furthermore, the break-up time, which is controlled by $C_2$ value, affects the SMD and the spray tip penetration, too. A low $C_2$ value has a small SMD overall value because the quick break-up causes a large number of the small droplet, on the other hand, a high $C_2$ value has a large SMD overall value because a large droplet remains a lot due to the late break-up. The wave length $\Lambda$ and wave growth rate depend on the local flow properties, it have the following Equations (12) and (13), respectively.

$$\Omega = \left(\frac{\rho_d r^3}{\sigma}\right)^{-0.5} \frac{0.34 + 0.38 \cdot We^{1.5}}{(1+Oh)(1+1.4 \cdot T^{0.6})} \tag{12}$$

$$\Lambda = 9.02 \cdot r \frac{(1 + 0.45 \cdot Oh^{0.5})(1 + 0.4 \cdot T^{0.7})}{(1 + 0.87 \cdot We^{1.67})^{0.6}} \tag{13}$$

Entering Ohnesorge number $Oh$ and Weber number $We$ as well as $T = Oh \cdot We^{0.5}$. As shown in Figure 4, the initial droplet size of the spray had a large diameter in the SMD scale because of the large diameter of the injector hole, however, the droplet size rapidly became to decrease by the break-up of a droplet. The comparison results of spray tip penetration can be confirmed as shown in Figure 5. Figure 5 shows the spray tip penetration characteristics under the different ambient pressure, and the spray tip penetration was defined as the distance from the injection start point to the most distant droplet. As shown in Figure 5, it was found that when the ambient pressure was increased in the experiment, the spray tip penetration was reduced because the drag force was raised by the high density and it disturbed the fuel injection progress. Furthermore, the spray cone angle was also thicker because the high drag force promoted the break-up of the injected fuel. When the results of spray tip penetration compared with numerical results, the error rate of spray tip penetration between the experimental and numerical results was less than 4.91 %. Besides, the difference of spray tip penetration according to the injection mass in the numerical results was less than 2.41 %. From these results, it can be said that the numerical model secured the reliability.

### 3.2. Effect of $CO_2$ Mole Fraction on the Spray Tip Penetration Characteristics

To investigate the effect of $CO_2$ mole fraction by simulated-EGR on the fuel droplet behavior in the CI engine, the obtained spray factors in the spray simulation were employed in the engine simulation.

Figure 6 shows the effect of $CO_2$ mole fraction by simulated-EGR on the visualization of spray tip penetration. It was found that the spray tip penetration became shorter with increasing the $CO_2$ mole fraction because the $CO_2$ (1.976 kg/m$^3$ at 0 °C and 1 atm) has a higher density than $N_2$ (1.251 kg/m$^3$ at 0 °C and 1atm). Therefore, the density in the cylinder raised with increasing the $CO_2$ mole fraction

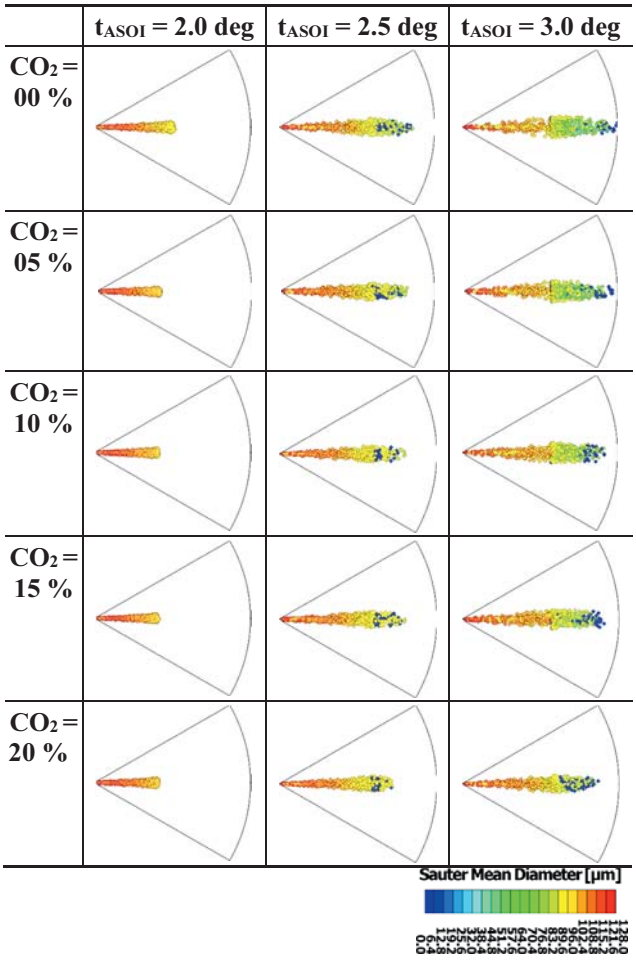


Figure 6. Effect of $CO_2$ mole fraction by simulated- EGR on the visualization of spray tip penetration ($P_{inj}$ = 100 MPa, $m_{inj}$ = 14 mg, $t_{eng}$ = BTDC 29 deg, $\phi$ = 0.68, 1200 rpm).

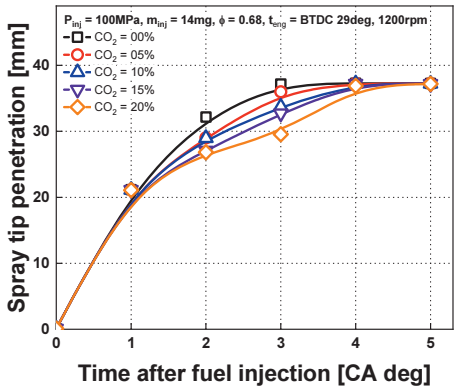


(a) Effect of $CO_2$ mole fraction ($t_{eng}$ = BTDC 29 deg)

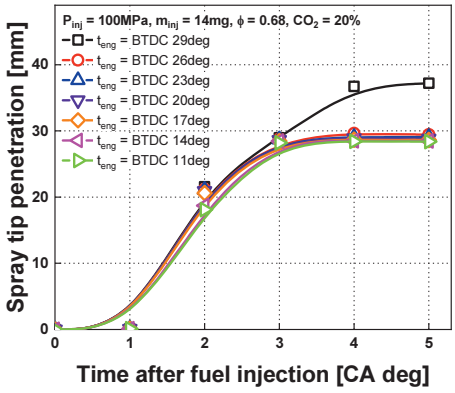


(b) Effect of start of energizing timing ($CO_2$ = 20 %)

Figure 7. Effect of $CO_2$ mole fraction by simulated- EGR on the spray tip penetration characteristics under the different start of energizing timing ($P_{inj}$ = 100 MPa, $m_{inj}$ = 14 mg, $\phi$ = 0.68, 1200 rpm).

under the same pressure, and it disturbed the progress of the fuel droplet. As a result, when the $CO_2$ mole fraction increased, the spray tip penetration was decreased due to the high density in the cylinder.

To exactly compare the spray tip penetration according to the $CO_2$ mole fraction, the spray tip penetration value according to the $CO_2$ mole fraction by simulated-EGR was compared as shown in Figure 7. Figure 7 shows the effect of $CO_2$ mole fraction by simulated-EGR on the spray tip penetration under the different start of energizing timing. In Figure 7 (a), it was observed that the spray tip penetrations are converged constant without the relation of $CO_2$ mole fraction because the distance from the start of injection to the reached place of fuel droplet is about 37.2 mm. In addition, in Figure 7 (b), when the start of energizing timing was BTDC 29 deg, the spray tip penetration was the longest because the injected fuel was able to reach the cylinder wall. The reason is that the piston was still rising from the lower due to the early injection. On the other hand, in the rest start of energizing timing, a relatively short distance from the start of injection place to the reached place of fuel droplet due to the rise of the piston.

The spray tip penetration was decreased with increasing the $CO_2$ mole fraction because the kinetic energy of fuel droplets was decreased as shown in Figure 8. Figure 8 shows the effect of $CO_2$ mole fraction on the maximum kinetic energy of one fuel droplet in the injected fuel, which was divided the whole kinetic energy on the injected fuel by the number of the total droplet. As described above, $CO_2$ has a higher density than $N_2$, and it induced to raise the total density in the cylinder, thereby suppressing the progress of fuel droplet. In addition, when the start of energizing timing retarded, although the kinetic energy according to the increment $CO_2$ mole fraction was reduced, the difference in spray tip penetration was reduced. Since the cylinder pressure was raised by retarding the start of energizing timing, it reduced the difference of kinetic energy, the fuel

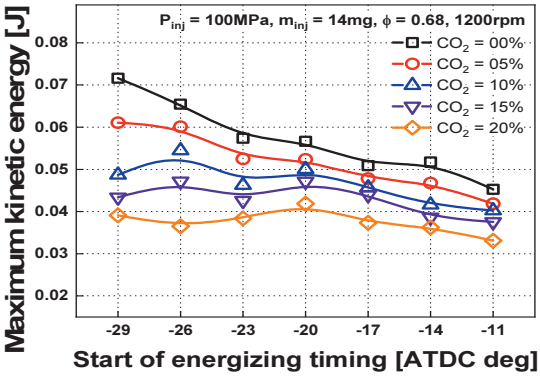


Figure 8. Effect of $CO_2$ mole fraction by simulated-EGR on the kinetic energy under the different start of energizing timing ($P_{inj}$ = 100 MPa, $m_{inj}$ = 14 mg, ϕ = 0.68, 1200 rpm).

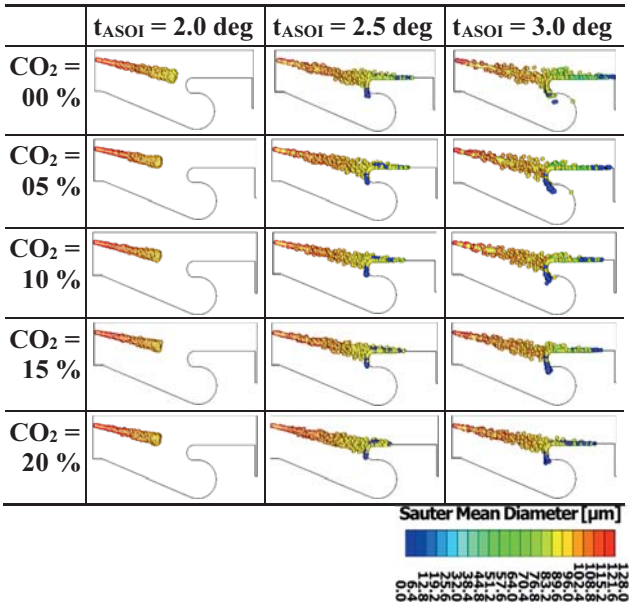


Figure 9. Effect of $CO_2$ mole fraction by simulated-EGR on the visualization of SMD ($P_{inj}$ = 100 MPa, $m_{inj}$ = 14 mg, $t_{eng}$ = BTDC 29 deg, ϕ = 0.68, 1200 rpm).

injection area was changed from squish volume to the piston bowl, which reduced the distance the fuel injection area. As a result, the increment of $CO_2$ mole fraction by simulated-EGR affected small to the spray tip penetration, however, it induced to reduce the kinetic energy of fuel droplet. Thus, it was judged that the difference in SMD, which is affected by kinetic energy, was could be cause.

### 3.3. Effect of $CO_2$ Mole Fraction on the SMD Characteristics

Figure 9 shows the effect of $CO_2$ mole fraction by simulated-EGR on the visualization of SMD. As shown in Figure 9, the small size fuel droplet was less distributed with increasing the $CO_2$ mole fraction because, as described above, the increased $CO_2$ mole fraction reduced the kinetic energy of fuel droplet, which affected not only the spray tip penetration, but also SMD.

To exactly analyze the effect of $CO_2$ mole fraction on the SMD characteristics under the different start of energizing timing in the engine simulation, the SMD characteristic is shown in Figure 10. The SMD values represent the time average value of each droplet SMD value in the cylinder. As shown in Figure 10 (a), when the $CO_2$ mole fraction by simulated-EGR raised, the SMD was slowly reduced, and the difference of value was from 74 % to 1,146 % because the high $CO_2$ mole fraction increased the density in the cylinder, which interrupted the injected fuel droplet progress. Even though the increased drag force, which was raised by the increased density in the cylinder, may decrease the SMD, it is believed that the break-up of fuel droplet was affected the kinetic energy of fuel droplet more than the drag force. As a result, it made that the injected fuel droplet had low kinetic energy, which induced to suppress the break-up of fuel droplet. Furthermore, when the start of energizing timing was BTDC 23 deg, it had a relatively large size of the fuel droplet as shown in Figure 10 (b) because the target of injected fuel was piston rim region. When the start of energizing timing advanced more or retarded more, the injected fuel introduced to the squish area or the bottom of the piston rim. However, when the start of energizing timing was BTDC 23 deg, the fuel was injected from the top of piston rim, hence a lot of fuel droplet was deposited, and then lots of liquid wall film was formed because the injected fuel flowed along with the piston bowl. The injected fuel hit the piston rim region, some of the injected fuel was broken-up to a very small size by the collision effect, which was quickly evaporated, and the other some of the injected fuel was deposited on the piston rim region. Thus, the relatively large size of the fuel droplet was maintained as shown in Figure 11.

Figure 11 shows the comparison of droplet number according to the size of fuel droplet under the different start of energizing timing. The SMD was defined that the sum of each fuel droplet size divided by the total number of droplets. Therefore, if the number of small size fuel droplet was less and the number of large size droplet, it has a large SMD value. When the start of energizing timing was BTDC 23 deg, it was observed that the total number of fuel droplet was the least, hence it could know that some of the fuel droplets may be deposited, and another some of the fuel droplet may be atomized by the collision effect, which quickly evaporated. Therefore, the number of small size droplets was less, and the number of large size droplets was relatively much than other starts of energizing timing,

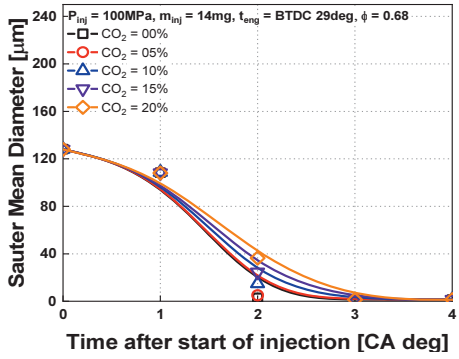


(a) Effect of $CO_2$ mole fraction ($t_{eng}$ = BTDC 29 deg)

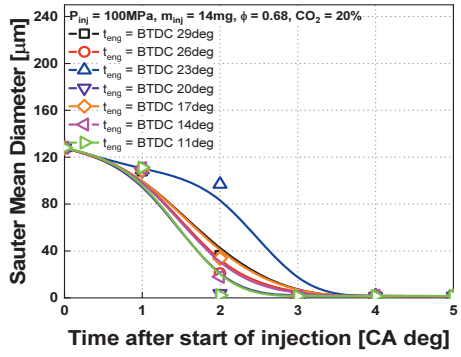


(b) Effect of start of energizing timing ($CO_2$ = 20 %)

Figure 10. Effect of $CO_2$ mole fraction by simulated- EGR on the overall SMD characteristics under the different start of energizing timing ($P_{inj}$ = 100 MPa, $m_{inj}$ = 14 mg, ϕ = 0.68, 1200 rpm).

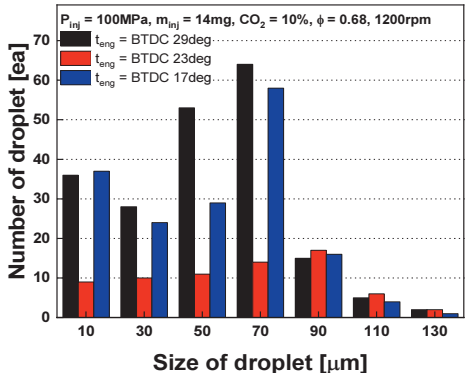


Figure 11. Comparison of droplet number according to the size of fuel droplet under the different start of energizing timing ($P_{inj}$ = 100 MPa, $m_{inj}$ = 14 mg, $CO_2$ = 10 %, ϕ = 0.68, 1200 rpm, $t_{ASOI}$ = 6 deg).

thereby it had relatively large SMD value. From these results, when the start of energizing timing was BTDC 23 deg, the representative emissions in CI engines such as soot and CO would be expected to decrease because the small size droplet which can be quickly evaporated by the collision effect induces the good combustion performance. In addition, good combustion performance may evaporate the deposited fuel, hence the $NO_X$ emissions could be also expected to reduce because the latent heat of vaporization absorbs the combustion temperature, and the combustion temperature will be decreased when the deposited fuel evaporated.

Consequently, it was found that the effect of $CO_2$ mole fraction on the SMD characteristics of the injected fuel droplet is difficult to observe after the start of energizing timing was BTDC 23 deg, and its effect can be observed before BTDC 26 deg and BTDC 29 deg. In addition, it was believed that factors affecting SMD characteristics were more influenced by the start of energizing timing than $CO_2$ mole fraction.

### 3.4. Effect of $CO_2$ Mole Fraction on the Evaporated Fuel Ratio Characteristics

The evaporated fuel ratio was defined that the evaporated fuel divided by the total amount of injected fuel. By comparing these results, it can be predicted the combustion performance such as ignition delay and so on. Figure 12 shows the effect of $CO_2$ mole fraction on the evaporated fuel ratio under the different the start of energizing timing. As 5 % $CO_2$ mole fraction increased, the evaporated fuel ratio was decreased by about 5 % because the $CO_2$ has a high specific heat (1.371 kJ/kg·K at 2,000 K) than $N_2$ (1.284 kJ/kg·K at 2,000 K) (Cengel and Boles, 2011). It means that the high specific heat of $CO_2$ suppressed the rising of the cylinder temperature, so the rising combustion temperature will also be expected to suppress. As well known, when the combustion performance is promoted, it induces to increase the combustion temperature, thereby the more $NO_X$ is formed. However, the high $CO_2$ mole fraction makes to suppress the rising of combustion temperature regardless of the combustion performance, so the formation of $NO_X$ will be restrained.

Figure 13 shows the effect of $CO_2$ mole fraction by simulated-EGR on the fuel mass fraction distributions in the cylinder. It was observed that when $CO_2$ mole fraction increased, the overall value of fuel mass fraction was less until $t_{ASOI}$ (the time after the start of injection timing) = 5 deg because, as described above, $CO_2$ has high specific heat which suppressed the rising of the cylinder temperature, it made to slowly evaporate the injected fuel droplet. However, after $t_{ASOI}$ = 8 deg, the overall value had a little high due to the late combustion start. After the combustion start, the value had similar. Moreover, the evaporated fuel ratio was slowly increased with retarding the start of energizing timing because the cylinder pressure was increased by retarding the start of energizing timing, which makes to increase the boiling point. However, when the start of energizing timing was BTDC 23 deg, the initial

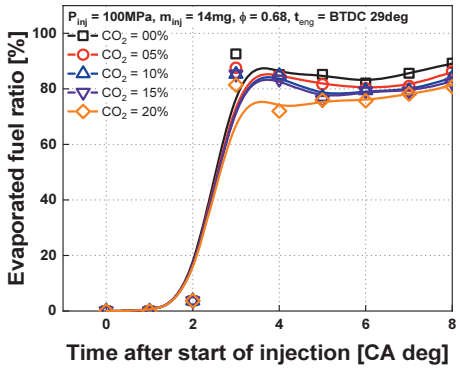


(a) Effect of $CO_2$ mole fraction ($t_{eng}$ = BTDC 29 deg)

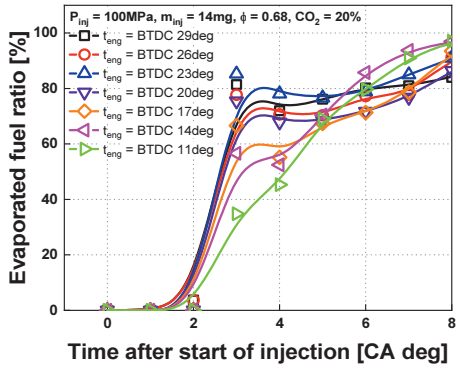


(b) Effect of start of energizing timing ($CO_2$ = 20 %)

Figure 12. Effect of $CO_2$ mole fraction by simulated-EGR on the evaporated fuel ratio under the different start of energizing timing ($P_{inj}$ = 100 MPa, $m_{inj}$ = 14 mg, ϕ = 0.68, 1200 rpm).

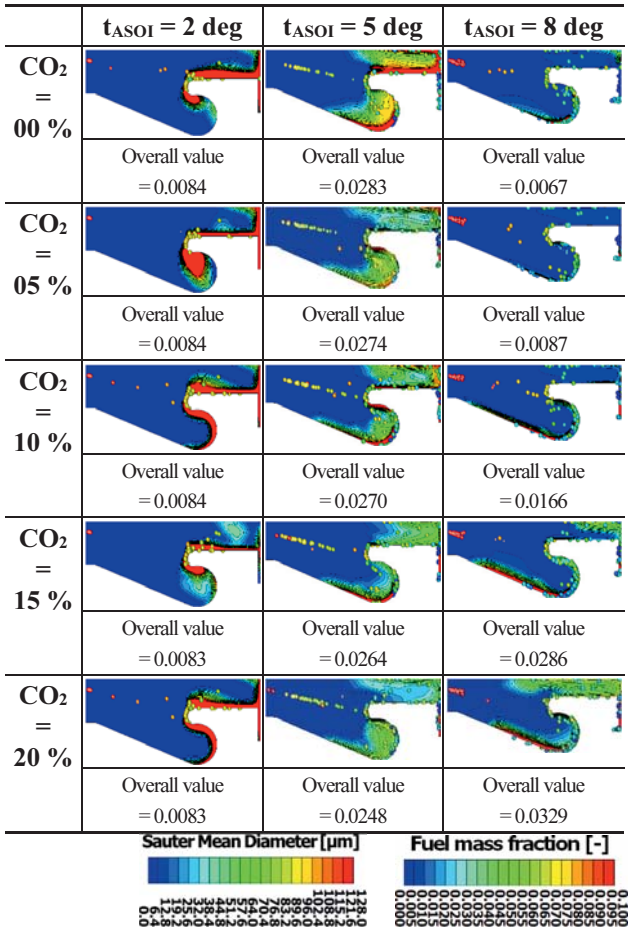


Figure 13. Effect of $CO_2$ mole fraction by simulated- EGR on the visualization of SMD ($P_{inj}$ = 100 MPa, $m_{inj}$ = 14 mg, $t_{eng}$ = BTDC 29 deg, ϕ = 0.68, 1200 rpm).

evaporated fuel ratio was observed to rapidly increase regardless of the $CO_2$ mole fraction as shown in Figure 12 (b).

Although some of the injected fuel droplets deposited at the piston rim region and flowed along with the piston bowl, the other some of the injected fuel droplet was actively caused the break-up by the collision effect.

As a result, it was expected that even though the liquid wall film was formed, the rapidly evaporated fuel by the collision effect promoted the combustion, and it made to evaporate the formed liquid wall film. So, when the liquid wall film evaporated, the combustion temperature may be absorbed by the latent heat vaporization, thereby the $NO_X$ emissions, which forms at the high temperature region, will be decreased. Furthermore, the representative emissions in CI engines such as soot and CO are expected to reduce because of the rapidly evaporated fuel by the collision effect and the promoted combustion by its results. As described above, although the rapidly evaporated fuel by the collision effect and the promoted combustion by its result are expected to simultaneously reduce the exhaust emissions such as $NO_X$ and incomplete combustion matter, it can negatively affect the engine performance. In this study, the effect of $CO_2$ mole fraction on the fuel droplet behavior in a cylinder under the early injection conditions was investigated, however the combustion performance and exhaust emission characteristics are also needed to exactly compare and analysis. Therefore, the engine performance and the exhaust emissions characteristics according to the $CO_2$ mole fraction under the early injection conditions will be studied in the future work.

## 4. CONCLUSION

This study was conducted to investigate the effect of $CO_2$ mole fraction controlled by simulated-EGR on fuel droplet behavior in the cylinder for simultaneous reduction of NO and soot in CI engine under the early injection conditions. The conclusions that can be obtained from this study are as follows.

(1) When the start of energizing timing advanced, and the $CO_2$ mole fraction increased, the spray tip penetration was decreased because the kinetic energy of the injected fuel droplet was reduced by the high density of $CO_2$.
(2) Even though the increased drag force, which was increased due to the high density in the cylinder by increasing the $CO_2$ mole fraction, may decrease the SMD, it is observed that the break-up of fuel droplet was more affected the kinetic energy of fuel droplet than the drag force.
(3) When the start of energizing timing was BTDC 23 deg, it had a relatively large size of the fuel droplet because the total number of fuel droplet was the least, hence it could know that some of the fuel droplets may be deposited, and another some of the fuel droplets are atomized by the collision effect, which was quickly evaporated.
(4) When the $CO_2$ mole fraction by simulated-EGR increased, the rich fuel mass fraction was distributed less until $t_{ASOI}$ was 5 deg because the cylinder temperature was slowly raised by the high specific heat of $CO_2$ which made to slowly evaporate the injected fuel.
(5) From these results, when the $CO_2$ mole fraction increased and the start of energizing timing was BTDC 23 deg, the $NO_X$ emission and soot emission were expected to simultaneously reduce because the rapidly evaporated fuel by the collision effect promoted the combustion, and it made to evaporate the formed liquid wall film, which evaporated and may absorb the combustion temperature by the latent heat vaporization.

**ACKNOWLEDGEMENT**–This work was supported by the research grant of the Kongju National University in 2018.

## REFERENCES

AVL GmbH (2013). Fire Version 2013.2 Spray Module Manual. AVL GmbH. Graz, Austria.

Bosch, W. (1966). The fuel rate indicator: A new measuring instrument for display of the characteristics of individual injection. *SAE Paper No.* 660749.

Cengel, Y. A. and Boles, M. A. (2011). *Thermodynamics: An engineering approach*. 7th edn. McGraw-Hill. New York, NY, USA.

Cha, J., Yoon, S., Lee, S. and Park, S. (2015). Effects of intake oxygen mole fraction on the near-stoichiometric combustion and emission characteristics of a CI (compression ignition) engine. *Energy*, **80**, 677–686.

Han, D. S., Lee, B. H., Bae, M. J., Chang, Y. J., Jeon, C. H. and Song, J. H. (2008). A numerical study on the spray characteristic of a marine diesel engine of injection spray angle and hole diameter. *Trans. KSME Spring Conf*., Jeongseon, Korea.

Heywood, J. B. (1988). *Internal Combustion Engine Fundamentals*. McGraw-Hill Education, New York, NY, USA.

Hountalas, D. T., Mavropoulos G. C. and Binder K. B. (2008). Effect of exhaust gas recirculation (EGR) temperature for various EGR rates on heavy duty DI diesel engine performance and emissions. *Energy* **33**, **2**, 272–283.

Karaeen, M. and Sher, E. (2011). Spray characteristics of diesel fuel containing dissolved $CO_2$. *Atomization and Sprays* **21**, **11**, 883–892.

Kökkülünk, G., Parlak, A., Ayhan, V. and Cesur, İ. (2012). Investigation of steam injection with exhaust gas recirculation (EGR) on a diesel engine. *3rd Int. Conf. Urban Sustainability, Cultural Sustainability, Green Development, Green Structures and Clean Cars (USCUDAR)*, Barcelona, Spain.

Ladommatos, N., Abdelhalim, S. M., Zhao, H. and Hu, Z. (1998). The effect of carbon dioxide in exhaust gas recirculation on diesel engine emissions. *Proc. Institution of Mechanical Engineers, Part D: J. Automobile Engineering* **212**, **1**, 25–42.

Lee, S. S. and Reitz, R. D. (2006). Spray targeting to minimize soot and CO formation in premixed charge compression ignition (PCCI) combustion with a HSDI diesel engine. *SAE Paper No*. 2006-01-0918.

Liu, Y., Xiang, Q., Wei, P., Zhang L., Yao, S., He, X. and Sun, H. (2020). Effects of carbon dioxide addition on diesel spray flame characteristics in oxygen-carbon dioxide atmospheres. *Fuel*, **276**, 118039.

Min, S. H., Suh, H. K. and Cha, J. (2020). Effect of simulated-EGR ($N_2$) on the distribution characteristics of equivalence ratio and the formation of exhaust emissions in a CI engine under early injection conditions. *Energy*, **193**, 116850.

Pandey, S. K, Vandana, S., Akella, S. S. and Ravikrishna, R. V. (2019). Potential of early direct injection (EDI) for simultaneous $NO_X$ and soot emission reduction in a heavy duty turbocharged diesel engine. *Applied Thermal Engineering*, **158**, 1–15.

Park, S., Reitz, R. D. and Kim, J. (2011). Combustion and emission characteristics of converging group-hole nozzle under lean engine operating conditions. *Fuel* **90**, **11**, 3259–3267.

Park, Y. and Bae, C. (2014). Experimental study on the effects of high/low pressure EGR proportion in a passenger car diesel engine. *Applied Energy*, **133**, 308–316.

Regulation (EC) No. 715/2007 (2007). European Parliament and of the Council. Official J. European Union. L 171/1-171/16.

Shi, X., Liu, B., Zhang, C., Hu, J. and Zeng, Q. (2017). A study on combined effect of high EGR rate and biodiesel on combustion and emission performance of a diesel

engine. *Applied Thermal Engineering*, **125**, 1272–1279.
Turns, S. (2012). *An Introduction to Combustion: Concepts and Applications.* 3rd edn. McGraw-Hill Education. New York, NY, USA.
Xiao, J., Huang, Z. and Qiao, X. (2008). Experimental study of the effects of carbon dioxide concentration in diesel fuel on spray characteristics. *J. Atomization and Sprays* **18**, **5**, 427–447.